Wahyu Widhi Dyatmika

Towards the Application of Ensemble Averaging in Spanwise Oscillating Wall Flow Control Analysis

SCHOOL OF AEROSPACE, TRANSPORT AND MANUFACTURING
Computational Fluid Dynamics

MSc
Academic Year: 2023 - 2024

Supervisor: Tamás Jozsa
25th August 2023

SCHOOL OF AEROSPACE, TRANSPORT AND MANUFACTURING
Computational Fluid Dynamics

MSc

Academic Year: 2023 - 2024

Wahyu Widhi Dyatmika

Towards the Application of Ensemble Averaging in Spanwise Oscillating Wall Flow Control Analysis

Supervisor: Tamás Jozsa
25th August 2024

This thesis is submitted in partial fulfilment of the requirements for the degree of MSc

Academic Integrity Declaration

I declare that:

- the thesis submitted has been written by me alone.

- the thesis submitted has not been previously submitted to this university or any other.

- that all content, including primary and/or secondary data, is true to the best of my knowledge.

- that all quotations and references have been duly acknowledged according to the requirements of academic research.

I understand that to knowingly submit work in violation of the above statement will be considered by examiners as academic misconduct.

Abstract

Acknowledgement

Contents

List of Figures

List of Tables

List of Symbols and Abbreviations

Abbreviations

CFD   Computational Fluid Dynamics

CF   Channel Flow

DNS   Direct Numerical Simulation

ISA   Inner-Scale Actuation

LES   Large-Eddy Simulation

NPS   Net Power Saving

OSA   Outer-Scale Actuation

PF   Pipe Flow

RANS   Reynolds Averaged Navier Stokes

Variables (Latin Letters)

E   Energy

e   Vector component

g   Gravitational vector

h   Height

L_o Integral Length Scale

n   Variable for showing time step

P   Pressure

Re   Reynolds number

t   Time

u   Velocity vector

$u. v, w$ Streamwise, wall-normal, and spanwise velocity, respectively

x, y, z Streamwise, wall-normal and spanwise direction, respectively

Variables (Greek Letters)

δ Characteristic length

η Kolmogorov length scale

κ Wave number

λ Minimal flow length

ν Kinematic viscosity

μ Dynamic viscosity

ρ Density

ϕ Transported quantity

Subscripts and Superscripts

$*$ Intermediate values

1

$+$	Wall-normal value
τ	Viscous quantities

1 Introduction

In the subject of fluid dynamics, flow control can massively influence the performance of the flow around or inside an object. Designing a flow control method requires intricate understanding of flow behaviours such as dynamics and turbulence. Designing a proper flow control can be essential for maximising the efficiency of the system.

1.1 Motivation

Climate change has been a driving factor for engineering design in the modern world [1]. The changes in climate pattern has proven to be detrimental to human and other living being. One of the causes of the climate change is the emission of energy generation process, such as carbon dioxide [2]. However, the need of creating more energy is indispensable as human population grows continuously, with energy requirement predicted to reach more than the triple of global energy requirement today [3]. This requires engineers to create a high performance solution with a consideration of efficiency in its operations. In aerospace sector, this approach is also used as the sector creates 2% of the total global emission, which is the largest among other means of transportation [4]. Generally in aerospace sector, high efficiency value can be reached by minimising drag, which generated from the viscous drag, as shown in Figure 1. The viscous drag can be practically reduced in a controlled manner using flow control strategies, offers a solution for a sustainable aerospace future [5].
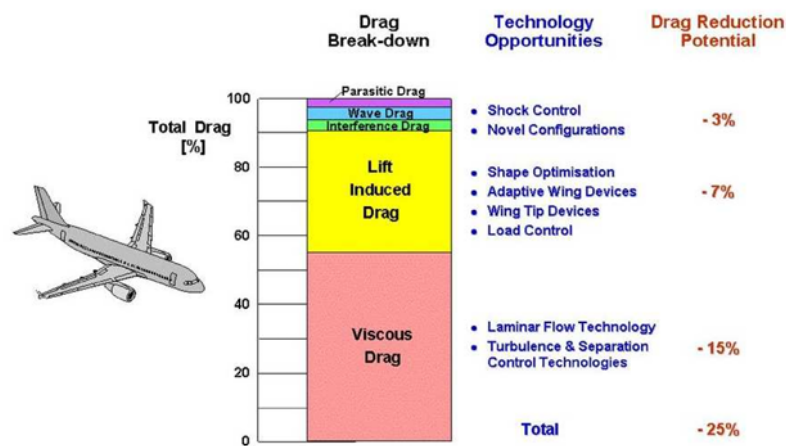
Figure 1: Drag and Reduction Potential in a General Aircraft [5]

Fluid flow control has been a major topic in fluid dynamics. Fluid flow control strategies have been implemented in various areas, such as aerospace, wind energy sector, industrial process designs, and water management [6]. The development of flow control methods was born from the understanding of the presence of turbulence in a fluid flow. Turbulence in a

moving flow can generally be denoted by the chaotic behaviour of the fluid [7], typically in the form of eddies or vortices. The interaction of the flow with itself, along with the solid object nearby can produce drag, which reduces the flow velocity and its ability to transport its properties [8]. In most systems, the drag can be detrimental as it can reduce the efficiency of the system. Because of that, flow control strategies are introduced to force the fluid to move in a regulated behaviour to decrease the drag produced in the system.

Currently, multiple strategies and approaches towards an efficient flow control system are studied. One of recent studies [9] suggests that an active flow control strategy in the form of spanwise wall oscillations can generate a positive net power saving value for high Reynolds number regimes. With the finding, a pathway for an industrial-wide application of oscillating wall flow control can be opened and hence a further studies are needed.

In order to further expand the spanwise wall oscillation flow control strategy, understanding the turbulence in the flow is of utmost importance, especially in the near wall region. Turbulence is the chaotic nature of a fluid flow, caused by "a complex interplay of multiple flow patterns occurring simultaneously, making difficult to model and predict accurately" [10]. Therefore, intricate physics modelling is generally required to completely simulate the turbulence in the flow, which growingly expensive in terms of computational cost as the Reynolds number increases [11]. In this paper, ensemble averaging is introduced as a solution for simulating intricate turbulence in a spanwise oscillating wall flow control analysis.

1.2 Literature Review

1.2.1 Physics of Wall Bounded Flow Turbulence

Turbulence can be defined as the swirling motion that happened randomly in the fluid flow [12]. Due to its randomness, turbulence phenomena can sometimes be too complicated and difficult to comprehend [13]. Therefore, most turbulence studies are focused on understanding the coherent structures, which are the regions with recognisable concentrated vorticity [14]. As seen in Figure 2, there are common structures in the flow region near the wall that is identifiable. The most prominent structure is the hairpin vortex, which indicated by a raising arch head with two streamwise-oriented legs [15].
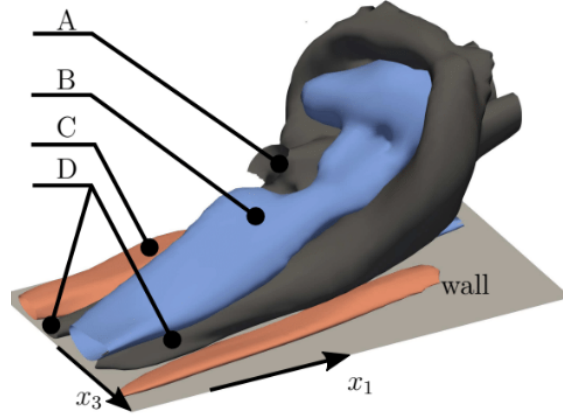
Figure 2: Near Wall Coherent Structures: A) Hairpin Vortex ; B) Low momentum region; C) high momentum region; D) counter-rotating quasi-streamwise vortices [16]

Several researches, such as the studies made by Wang [15] and Alfonsi [17] explained how the hairpin vortices generated. First, the legs of the hairpin vortices, which consist of two quasi-streamline, counter-rotating vortices are interacted with each other. These vortices rises to the area with lower shear magnitudes, which decreases the vorticity magnitude. With the opposing rotational direction, the coalescence of two vortical structures are occurred and the hairpin vortices are generated. Inside the vortex, low momentum region is generated. Conversely, the high momentum region is generated outside the two counter-rotating vortices.

Other than the physical structures, the spectral analysis is also commonly conducted to understand the turbulence phenomena. Generally, spectral analysis involves analysing the turbulence through the wave energy distribution in the structures [18]. In order to visualise the energy distribution, the Kolmogorov spectrum is used, as shown in the Figure 3.

Based on Brennen [19], there are 3 main regions in the spectrum. The first is the integral region, or commonly known as the energy containing range. This characterises the overall size of the largest eddies, which contains the energy in the flow. These large scale structures are responsible for transfering energy to the from the external forces to the smaller structures in the turbulent flow. The energy is then cascades to the smaller scales through the inertial region. The energy spectrum in this region follows a power law distribution:

$$E(k) \propto k^{\frac{5}{3}} \tag{1}$$

Where k is wave number. Afterwards, the energy cascades to the smallest scales, which are in the Kolmogorov scales. In this scales, the viscosity dominates and the kinetic energy is transfered to heat energy.
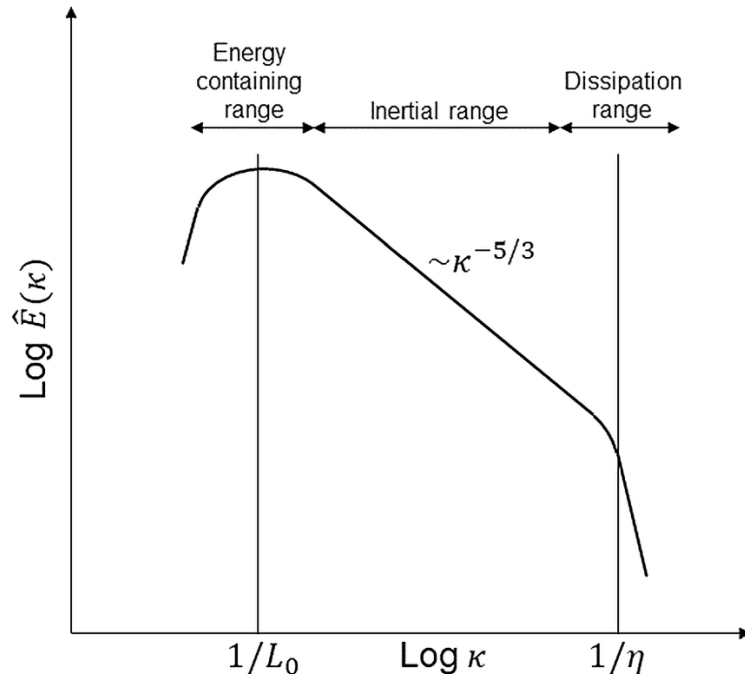
Figure 3: Typical Energy Spectrum in a Flow [20]

1.2.2 Spanwise Oscillating Wall Flow Control

Flow control can be defined as the method of altering the flow to a desired state or path [21]. Typically, there are two types of flow control methods, as stated by Ricco [22]. The first method is the passive flow control, which requires no actuation or movement in the system, thus no external energy required to control the fluid flow. The second method is the active flow control. Contrary to its passive counterpart, the active flow control requires energy to actuate a motion in a flow.

Due to the certain energy consumption, most of the study regarding active flow control are circulated around the strategy to create a motion that has a positive net power saving. The same trend has been observed for spanwise oscillating wall method, which requires actuation to create an oscillation in the near wall region. The concepts and methods are documented in Table 1.

Table 1: Experimental and Computational Studies of Spanwise Oscillating Wall Flow Control

References	Geometry	Methodology	Reynolds Number	NPS_{max} (%)
Marusic et al. (2021) [9]	CF	Experimental: Hot-wire anemometry	$Re_\tau = 6000$	~7
			$Re_\tau = 12800$	~2
		Computational: LES (dynamic Smagorinsky)		
Gatti and Quadrio (2016) [23]	CF	Computational: DNS	$Re_\tau = 200$	5.3 ± 0.24
			$Re_\tau = 1000$	3.9 ± 0.31
Quadrio et al. [24]	CF	Computational: DNS	$Re = 4760$	5
Auteri et al. (2010) [25]	PF	Experimental, with DNS comparison from [24]	$Re = 4760$	17
Viotti et al. (2009) [26]	CF	Computational: DNS	$Re_\tau = 200$	23
Chandran et al. (2023) [27]	CF	Experimental: Drag Balance and Hot Wire Anemometry	$4500 \leq Re_\tau \leq 150000$	ISA: -40 OSA: 5-10
Deshpande et al. (2024) [28]	CF	Computational: DNS	$Re_\tau \approx 300$	Not reported
Nguyen et al. (2021) [29]	CF (with square bar)	Computational: DNS	$Re_\tau = 218$	0.8
Ricco et al. (2012) [30]	CF (rough wall)	Computational: DNS	$Re_\tau = 200$	Not reported

The key trend from the results is the NPS value is dependent from various factors. It is apparent from the studies that the NPS value of of the flow control decreases as the Reynolds number increases [23] [24]. Other than that, the net power saving also relies on the wave function applied. From the studies, it can be seen that the net power saving is positive when the wave function of the oscillating wall matches the large-scale eddies inside the flow [9][27].

Based on the table, a simple channel flow is the most common base case to test the effectivity of flow control. This is due to the simplicity of the flow modelling as the case only has two wall surface, generally placed on the top and the bottom of the domain. The domain surfaces on the side are assumed to be free surfaces [31]. To the boundary condition assignment, the effect of the wall in the flow will be easier to analyse without having to take account the wall perpendicular to the wall of interest.

1.2.3 Turbulence Modelling

Solving turbulence is required in order to create a good model of a fluid flow. This is because turbulence is highly related to the transport of mass, energy, and other values in the flow [32]. However, variety in the temporal and spatial scale of turbulence oftentimes requires high computational power [33]. To alleviate the excessive computational power, turbulence modelling is often used, generally in the form of Reynolds Averaged Navier Stokes (RANS) [34]. However, due to the nature of the modelling, some simplifications leads to information loss, especially regarding the energy cascade to the small scales [35]. Other approach that can be done is using the Large Eddy Simulation (LES). LES method solves large eddies directly, but uses modelling to solve the small eddies [36]. This way, high accuracy can be obtained for the large structures, while maintaining low computational expenses. However, similar to RANS modelling, inaccuracy can occur in small-scale turbulence [37].

In cases where the effect of small-scales turbulence are heavily considered, turbulence modelling is fully disregarded. This means that the Navier-Stokes equations are directly solved [38]. These method of solving the fluid flow is termed Direct Numerical Simulation (DNS). Ideally, DNS should be performed with spatial resolution at least as large as the Kolmogorov scale, which the smallest eddies that can be produced by the flow [39]. However, the fine grid resolution will make the analysis prohibitively expensive. Therefore, lower resolution usually preferred to DNS methods.

1.2.4 Generalised Richardson Extrapolation

In a computational analysis, the domain settings may change the value of the results. The finer the settings is, the higher the quality of the results. However, finer results require high

computational resources which limits the resolution of the model. To counter the problem. the Richardson extrapolation is usually used. Richardson extrapolation can be defined as the approximation of the ideal value of convergent value using [40]:

$$f_{h=0} \overset{\sim}{=} \frac{4}{3}f_1 - \frac{1}{3}f_2 \tag{2}$$

However, most of the application of Richardson extrapolation are limited to the spatial convergence. The novel method of Richardson extrapolation includes temporal and domain size to determine the best resolution of a computational case. The combined resolution is expressed as:

$$NormalisedResolution = \frac{\Delta x_e^{current}}{\Delta x_e^{finest}} \frac{\Delta t^{current}}{\Delta t^{finest}} \frac{t_{tot}^{finest}}{t_{tot}^{current}} \frac{L_e^{finest}}{L_e^{current}} \tag{3}$$

1.2.5 Sample Averaging

To understand the overall trend of a numerical result, the result must be averaged. The averaging is normally done using two different method. First is time averaging, which is the more common practice in CFD analysis. Time averaging involves obtaining the flow properties such as velocities and pressure over a long period of time. After that, the flow value is averaged. This way, the fluctuations during a transient analysis can be avoided, thus making further calculations easier [41]. Because of this, the time-averaging method is popular in steady-state analysis [42]. However, the long period sampling time requires high computational resources, especially when high-fidelity approaches are used [43].

The alternative method of sample averaging is using the ensemble averaging. By definition, ensemble averaging requires "averaging over numerous independent simulations"[44]. Ensemble averaging decreases the requirement of computational power, thus making the analysis more efficient, especially in high Reynolds number [43]. Currently, the method is not popular in fluid dynamics, but the method is commonly used in molecular dynamics, where time-averaging is very costly to perform [45].

In a practical sense, time and ensemble averaging have a possibility to have the correlating result to one and another. This commonly referred as ergodicity, a statistical property that exhibits that the system has the equal value of ensemble and time averaging [46]. Turbulent flow, as shown in recent study [47], has known to be ergodic. Therefore, turbulent flow analysis can benefit from both methods without sacrificing the result generation.

1.2.6 Xcompact3d

The research mainly uses Xcompact3d to solve the fluid flow. Xcompact3d is a FORTRAN 90 based open-source software purposed to simulate incompressible fluid flows [48]. The software uses high order compact schemes [49], which utilises shortened version of high order schemes. This way, the analysis will still satisfy the need of high resolution of high-order schemes, while maintaining simplicity of low-order schemes [50], making the compact schemes a powerful and efficient tool to solve turbulence.

With the higher order schemes, the simulation can run high fidelity schemes to solve the viscous terms in the Navier-Stokes equation. The two models that are available to use in Incompact3d is Large Eddy Simulation (LES) and Direct Numerical Simulation (DNS) [49]. As the section 1.2.3 suggests, both methods are preferable when it comes to analysing turbulence in detail.

1.2.7 Knowledge Gap

Current spanwise oscillating wall flow control research lacks a thorough analysis in high Reynolds number. To conduct flow control studies using CFD, researchers must analyse turbulence in great depth, usually using LES or DNS analysis. This leads to high computational expenses. The requirement of high computational power also increased with the increase of Reynolds number. Moreover, the studies conducted uses time–averaged approaches, further pushing the need of ensemble averaging approach as an alternative approach. With this study, future study can hopefully be conducted at a high Reynolds number region that could not be done before.

1.3 Aim and Objectives

The aim of the study is to analyse the effectivity of ensemble averaging in numerical analysis of spanwise oscillating wall flow control.

With this aim, the objectives can be set as the steps to achieve the aim set. The objectives are set as follows:

- Generate a channel flow grid as a case for the study
- Generate a generalised Richardson extrapolation by changing the spatial and temporal resolution
- Conduct flow simulations of the channel flow with and without spanwise oscillating wall flow control using DNS
- Generate and compare the time and ensemble averaging results using post-processing methods

1.4 Synopsis

The thesis is arranged to be in a form as follows. Section 2 provides the theoretical background and the methodology for the thesis. The governing equations, along with the supporting equations used in the numerical simulations are thoroughly explained. Moreover, the computational procedures, including geometry and mesh generations, simulations settings and post processing methods are introduced in this section.

Results obtained from the analysis is displayed in Section 3. The discussion is then served as the rationale of the result. Several figures and tables are displayed as a summary for the result and an aid for understanding the phenomena behind the flow condition. Section 4 presents the conclusions of the current study and recommendations for future studies.

2 Methodology

2.1 Flow Problem of Interest

To understand the effect of oscillating wall flow control to the effect of the flow, a case must be formulated as an example case. Generally, the case used is a canonical flow problem, which the information and data are abundantly accessible and can easily compared to one and another. Therefore, the turbulence phenomena can be throughly examined. In this study, a simple double periodic channel flow problem is used to be analysed for the oscillating wall flow control problem. Double periodic channel flow cases utilises periodic boundary conditions on two sets of planes: spanwise and streamwise planes.

The first thing to do when simulating a double periodic channel flow problem is to determine the requirement of the channel flow domain size. The size of the domain must be meticulously determined to minimise the computational expenses but ensuring all of the necessary turbulence structures are captured appropriately. The minimum size of the double periodic channel flows are commonly referred as the minimal flow unit [51], shown in Figure 4.
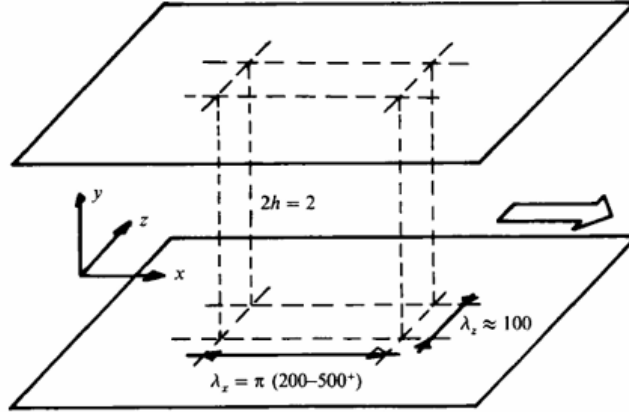
Figure 4: Minimal Flow Unit of a Double Periodic Channel Flow [51]

The length of the minimal flow unit is defined in a wall flow unit, denoted by the (+) sign. The (+) sign is a normalisation of the quantity using the turbulent boundary layers, formulated as:

$$+ = \frac{\nu}{u_\tau} \tag{4}$$

Where u_τ is a function of wall friction, defined as [52]:

$$u_\tau = \sqrt{\frac{\tau_w}{\rho}} \tag{5}$$

τ_w is related to the Reynolds numbers and the velocity gradient to the normal direction, stated as [53]:

$$\tau_w = \frac{\partial u}{\partial y} Re \tag{6}$$

Re is the dimensionless number which displays the ratio between the inertial and viscous forces, expressed as [54]:

$$Re = \frac{v\delta}{\nu} \tag{7}$$

For study in turbulence, friction Reynolds numbers are more commonly used due to its relevance to the near wall turbulence. The equation of the friction Reynolds number is displayed below [52].

$$Re_\tau = \frac{u_\tau \delta}{\nu} \approx 0.09(2Re)^{0.88} \tag{8}$$

For the base case, the Reynolds number are defined as $Re_\tau = 180$. The quantity is chosen due to the availability of DNS channel flow data [55] and the data from Xcompact3D [48]. The fluid properties data is shown in the Table 2 below.

Table 2: Fluid Properties

Re_τ	**Re**	**u**	ρ	ν
180	2819.294	1	1	0.00035

2.2 Theoretical Background

2.2.1 Governing Equations of Incompressible Fluid Flow

In a general fluid flow, there are two equations that are used for the equation[56]. The first, continuity equation is expressed as:

$$\frac{\partial P}{\partial t} + \nabla(\rho \mathbf{u}) = 0 \tag{9}$$

The second, is the momentum equation, which are commonly mentioned as the Navier-Stokes equation, is expressed as:

$$\underbrace{\rho \frac{\partial \mathbf{u}}{\partial t}}_{\text{I.}} + \underbrace{\rho(\mathbf{u} \cdot \nabla)\mathbf{u}}_{\text{II.}} = \underbrace{\rho \mathbf{g}}_{\text{III.}} - \underbrace{\nabla P}_{\text{IV.}} + \underbrace{\mu \nabla^2 \mathbf{u}}_{\text{V.}} + \underbrace{\frac{\mu}{3}\nabla(\nabla \mathbf{u})}_{\text{VI.}} \tag{10}$$

Where

$$\mathbf{u} = u\mathbf{e_x} + v\mathbf{e_y} + w\mathbf{e_z} \tag{11}$$

13

There are six members in a full on Navier-Stokes Equation. The first member is the unsteady term, showing the change of the fluid velocity over time. The second member is the convective-advective term, showing the transport of properties in the flow. The third term, gravity force field, displays the effect of gravity in the flow, The fourth term is the pressure gradient, showing the change of pressure in the fluid. The fifth term, the diffusion term, determines how the viscous diffusion and dissipation affecting the flow. Lastly, the sixth term, shows the compressibility effect due to the viscous terms.

In a low Reynolds number case such as defined in Section 3.1, the fluid becomes incompressible, which transforms both governing equations[57]. For the continuity equation, the expression simplifies into:

$$\nabla \mathbf{u} = 0 \tag{12}$$

On the other hand, the momentum equation changes by dropping the compressibility term. Additionally, the momentum equation can be modified by normalising every term to density, as density remains constant in incompressible flow.

$$\frac{\partial \mathbf{u}}{\partial t} + (\mathbf{u} \cdot \nabla)\mathbf{u} = \mathbf{g} - \frac{1}{\rho}\nabla P + \nu\nabla^2\mathbf{u} \tag{13}$$

2.2.2 Fractional Step Method

In incompressible flow, the density remains constant while the pressure changes. Therefore, the equation of state is not applicable [57], hence pressure and velocity equation must be calculated together in a coupled equation. In Xcompact3D, Chorin's Fractional Step Method is used [58]. In Fractional Step method, there are three steps that is conducted to couple the pressure and velocity variables [59]. The first step utilises intermediate velocity field, which is expressed as:

$$\mathbf{u}^* = \mathbf{u}^n + \Delta t \left[\mathbf{g} + \nu\nabla^2\mathbf{u} - (\mathbf{u}\nabla)\mathbf{u}\right]^{(n)} \tag{14}$$

Then, the second step is conducted to solve the pressure equation as follows:

$$\nabla^2 P^{n+1} = \frac{\rho}{\Delta t}\left[\nabla \mathbf{u}^*\right] \tag{15}$$

Finally, the third step is to update the velocity.

$$\mathbf{u}^{n+1} = u^* - \frac{\Delta t}{\rho}\nabla P^{n+1} \tag{16}$$

14

2.2.3 Spatial Discretisation

2.2.4 Temporal Discretisation

Other than the spatial discretisation, temporal discretisation must also be applied to calculation so the numerical simulation can be progressed to the next time step. For nearly all of the time discretisation, the third-order Adam-Bashforth equation is used. The third order Adam-Bashforth scheme is an explicit scheme that uses one equation to progress the time step of the calculation [60], displayed as:

$$\phi^{n+1} - \phi^n = \frac{\Delta t}{12}[23F^n - 16F^{n+1} + 5F^{n-2}] \tag{17}$$

Where

$$F^n = \mathbf{u}^n \phi^n$$
$$F^{n-1} = \mathbf{u}^{n-1} \phi^{n-1}$$
$$F^{n-2} = \mathbf{u}^{n-2} \phi^{n-2}$$

For the diffusion term in the wall-normal direction, the implicit Crank-Nicolson equation is also used for the time discretisation. The temporal discretisation for the y-diffusion term can be expressed as:

$$\left(\nu \frac{\partial^2 v}{\partial y^2} \right)^{n+\frac{1}{2}} = \frac{1}{2} \left(\nu \frac{\partial^2 v^{n+1}}{\partial y^2} + \nu \frac{\partial^2 v^n}{\partial y^2} \right) \tag{18}$$

2.3 Computational Procedures

2.3.1 Grid Generation

For the entirety of the study, the cartesian structured grid is used. The entire model is discretised into a system of hexahedral-shaped elements with eight nodes connecting to each other [61]. In a simple canonical flow as this study, the structured hexahedral grid is favoured due to the the efficiency of the shape in terms of filling the spaces, as well as the ability of minimising diffusion when transfering the properties from an element to another [62]. Additionally, the simple connectivity of the elements makes the grid model simple to program [63].

To capture the near-wall turbulence, the size of the grid near the wall must be decreased. However, just uniformly decrease the size of the grid may cause an unnecessary computational expense as the flow on the centre of the channel flow do not have substantial gradient or turbulence structures. To compensate the problem, a stretching algorithm is introduced

in the Xcompact3d program [50], developed from [64] and [65]. First, the domain must be expressed in physical coordinate y and computational coordinate s.

$$y = h(s), 0 \le s \le 1, 0 \le y \le L_y \tag{19}$$

The y-height of each members can be defined as

$$h = \frac{L_y\sqrt{\beta}}{\gamma\sqrt{\alpha}\sqrt{\alpha\beta+1}} \left\{ \tan^{-1}\left(\frac{\sqrt{\alpha\beta}+1 \tan(\pi(\gamma s+\delta))}{\sqrt{\alpha}\sqrt{\beta}} \right) + \pi \left[H\left(s - \frac{1-2\delta}{2\gamma} \right) + H\left(s - \frac{3-2\delta}{2\gamma} \right) \right] - \tan^{-1}\left(\frac{\sqrt{\alpha\beta}+1 \tan(\pi\delta)}{\sqrt{\alpha}\sqrt{\beta}} \right) \right\} \tag{20}$$

On a default channel case in Xcompact3d, the refinement are conducted solely for the wall. Therefore, $\gamma = 1$ and $\delta = \frac{1}{2}$. For all the case, β is set to 0.259065151.

2.3.2 Numerical Simulations: Settings

2.3.3 Numerical Simulations: Simulations Campaign

3 Results and Discussion

3.1 Flow Problem of Interest

3.1.1 Aerodynamic Efficiency

3.1.2 Flow Physics

3.1.3 Pressure and Moment Coefficients

3.2 Viscous Flow

3.3 Off-Design Conditions

4 Conclusions and Recommendations

4.1 Conclusions

4.2 Recommendations for Future Work

References

[1] E. Douglas, J. Jacobs, K. Hayhoe, *et al.*, "Progress and challenges in incorporating climate change information into transportation research and design," *Journal of Infrastructure Systems*, vol. 23, no. 4, p. 04 017 018, 2017. DOI: 10.1061/(ASCE)IS. 1943-555X.0000377. eprint: https://ascelibrary.org/doi/pdf/10.1061/%28ASCE% 29IS.1943-555X.0000377. [Online]. Available: https://ascelibrary.org/doi/abs/10. 1061/%28ASCE%29IS.1943-555X.0000377.

[2] Met Office, *Causes of climate change*. [Online]. Available: https://www.metoffice. gov.uk/weather/climate-change/causes-of-climate-change.

[3] IRENA, *Investment Needs of USD 35 trillion by 2030 for Successful Energy Transition*, 2023. [Online]. Available: https://www.irena.org/News/pressreleases/2023/ Mar/Investment-Needs-of-USD-35-trillion-by-2030-for-Successful-Energy-Transition.

[4] IEA, *Tracking clean energy progress 2023*. [Online]. Available: https://www.iea. org/reports/tracking-clean-energy-progress-2023.

[5] A. Abbas, G. Bugeda, E. Ferrer, *et al.*, "Drag reduction via turbulent boundary layer flow control," *Science China Technological Sciences*, vol. 60, pp. 1281–1290, 9 Sep. 2017, ISSN: 18691900. DOI: 10.1007/s11431-016-9013-6.

[6] C. Airiau, R. King, and B. R. Noack, *Open invited track : Flow control strategies and applications*, 2016.

[7] R. Benzi and F. Toschi, "Lectures on turbulence," *Physics Reports*, vol. 1021, pp. 1–106, Jun. 2023, ISSN: 03701573. DOI: 10.1016/j.physrep.2023.05.001.

[8] W. Bell, "The influence of turbulence on drag," *Ocean Engineering*, vol. 6, pp. 329–340, 3 Jan. 1979, ISSN: 00298018. DOI: 10.1016/0029-8018(79)90021-0.

[9] I. Marusic, D. Chandran, A. Rouhi, *et al.*, "An energy-efficient pathway to turbulent drag reduction," *Nature Communications*, vol. 12, 1 Dec. 2021, ISSN: 20411723. DOI: 10.1038/s41467-021-26128-8.

[10] T. Alberti, R. Benzi, and V. Carbone, "Why (still) studying turbulence in fluids and plasmas?" *Perspectives of Earth and Space Scientists*, vol. 4, 1 Dec. 2023, ISSN: 2637-6989. DOI: 10.1029/2023cn000215.

[11] S. Chen, S. Sammak, P. Givi, J. P. Yurko1, and X. Jia, "Reconstructing high-resolution turbulent flows using physics-guided neural networks," Sep. 2021. [Online]. Available: http://arxiv.org/abs/2109.03327.

[12] K. R. Sreenivasan, "Fluid turbulence," *Reviews of Modern Physics*, vol. 71, pp. 383–395, 2 1999.

[13] A. K. F. Hussain, "Coherent structures and turbulence," *Journal of Fluid Mechanics*, vol. 173, pp. 303–356, 1986, ISSN: 14697645. DOI: 10 . 1017 / S0022112086001192.

[14] H. E. Fiedler, "Coherent structures in turbulent flows," *Prog. Aerospace Sci.*, vol. 25, pp. 231–269, 1988.

[15] Y. Wang, W. Huang, and C. Xu, "On hairpin vortex generation from near-wall streamwise vortices," *Acta Mechanica Sinica/Lixue Xuebao*, vol. 31, pp. 139–152, 2 May 2015, ISSN: 05677718. DOI: 10.1007/s10409-015-0415-8.

[16] T. I. Józsa, *Drag reduction by passive in-plane wall motions in turbulent wall-bounded flows[ph.d thesis]*, 2019.

[17] G. Alfonsi, "Coherent structures of turbulence: Methods of eduction and results," *Applied Mechanics Reviews*, vol. 59, pp. 307–323, 1-6 2006, ISSN: 00036900. DOI: 10.1115/1.2345370.

[18] Y. Fan and W. Li, "Spectral analysis of turbulence kinetic and internal energy budgets in hypersonic turbulent boundary layers," *Phys. Rev. Fluids*, vol. 8, p. 044 604, 4 Apr. 2023. DOI: 10.1103/PhysRevFluids.8.044604. [Online]. Available: https://link.aps.org/doi/10.1103/PhysRevFluids.8.044604.

[19] C. Brennen, "Turbulence spectra and scales," in California Institute of Technology, 2004.

[20] T. Kalmár-Nagy and B. D. Bak, "An intriguing analogy of kolmogorov's scaling law in a hierarchical mass–spring–damper model," *Nonlinear Dynamics*, vol. 95, pp. 3193–3203, 4 Mar. 2019, ISSN: 0924-090X. DOI: 10.1007/s11071-018-04749-x.

[21] M. Jahamiri, *Active flow control: A review*, 2010.

[22] P. Ricco, M. Skote, and M. A. Leschziner, "A review of turbulent skin-friction drag reduction by near-wall transverse forcing," *Progress in Aerospace Sciences*, vol. 123, May 2021, ISSN: 03760421. DOI: 10.1016/j.paerosci.2021.100713.

[23] D. Gatti and M. Quadrio, "Reynolds-number dependence of turbulent skin-friction drag reduction induced by spanwise forcing," *Journal of Fluid Mechanics*, vol. 802, pp. 553–582, Sep. 2016, ISSN: 14697645. DOI: 10.1017/jfm.2016.485.

[24] M. Quadrio, P. Ricco, and C. Viotti, "Streamwise-travelling waves of spanwise wall velocity for turbulent drag reduction," *Journal of Fluid Mechanics*, vol. 627, pp. 161–178, 2009, ISSN: 14697645. DOI: 10.1017/S0022112009006077.

[25] F. Auteri, A. Baron, M. Belan, G. Campanardi, and M. Quadrio, "Experimental assessment of drag reduction by traveling waves in a turbulent pipe flow," *Physics of Fluids*, vol. 22, 115103 Aug. 2010. DOI: 10.1063/1.3491203. [Online]. Available: http://arxiv.org/abs/1008.2584%20http://dx.doi.org/10.1063/1.3491203.

[26] C. Viotti, M. Quadrio, and P. Luchini, "Streamwise oscillation of spanwise velocity at the wall of a channel for turbulent drag reduction," *Physics of Fluids*, vol. 21, pp. 1–9, 11 2009, ISSN: 10706631. DOI: 10.1063/1.3266945.

[27] D. Chandran, A. Zampiron, A. Rouhi, *et al.*, "Turbulent drag reduction by spanwise wall forcing. part 2. high-reynolds-number experiments," *Journal of Fluid Mechanics*, vol. 968, Jul. 2023, ISSN: 14697645. DOI: 10.1017/jfm.2023.498.

[28] R. Deshpande, A. G. Kidanemariam, and I. Marusic, "Pressure drag reduction via imposition of spanwise wall oscillations on a rough wall," *Journal of Fluid Mechanics*, vol. 979, Jan. 2024, ISSN: 0022-1120. DOI: 10.1017/jfm.2023.1062.

[29] V. T. Nguyen, P. Ricco, and G. Pironti, "Separation drag reduction through a spanwise oscillating pressure gradient," *Journal of Fluid Mechanics*, vol. 912, 2021, ISSN: 14697645. DOI: 10.1017/jfm.2020.1124.

[30] P. Ricco, C. Ottonelli, Y. Hasegawa, and M. Quadrio, "Changes in turbulent dissipation in a channel flow with oscillating walls," *Journal of Fluid Mechanics*, vol. 700, pp. 77–104, Jun. 2012, ISSN: 14697645. DOI: 10.1017/jfm.2012.97.

[31] D. D. Apsley, *Flow in Pipes and Channels [Lecture Notes]*, 2023. [Online]. Available: https://personalpages.manchester.ac.uk/staff/david.d.apsley/lectures/hydraulics2/t2.

[32] The TrEnCh Project, "Turbulence and fluid flow," in University of Washington, 2023.

[33] K. Duraisamy, G. Iaccarino, and H. Xiao, "Turbulence modeling in the age of data," *Annual Review of Fluid Mechanics*, vol. 51, pp. 357–377, 1 Jan. 2019, ISSN: 0066-4189. DOI: 10.1146/annurev-fluid-010518-040547.

[34] N. A. C. Sidik, S. N. A. Yusuf, Y. Asako, S. B. Mohamed, and W. M. A. A. Japa, "A short review on rans turbulence models," *CFD Letters*, vol. 12, pp. 83–96, 11 Nov. 2020, ISSN: 21801363. DOI: 10.37934/cfdl.12.11.8396.

[35] R. H. Bush, T. Chyczewski, K. Duraisamy, B. Eisfeld, C. L. Rumsey, and B. R. Smith, *Recommendations for future efforts in rans modeling and simulation*, 2020.

[36] Y. Zhiyin, "Large-eddy simulation: Past, present and the future," *Chinese Journal of Aeronautics*, vol. 28, pp. 11–24, 1 Feb. 2015, ISSN: 10009361. DOI: 10.1016/j.cja.2014.12.007.

[37] P. Mason, "Large-eddy simulation: A critical review of the technique," *Quarterly Journal of Royal Meteorological Society*, vol. 120, pp. 1–26, 1994.

[38] P. Moin and K. Mahesh, "Direct numerical simulation: A tool in turbulence research," *Annual Review of Fluid Mechanics*, vol. 30, pp. 539–578, 1998, ISSN: 00664189. DOI: 10.1146/annurev.fluid.30.1.539.

[39] J. Boschung, F. Hennig, M. Gauding, H. Pitsch, and N. Peters, "Generalised higher-order kolmogorov scales," *Journal of Fluid Mechanics*, vol. 794, pp. 233–251, May 2016, ISSN: 14697645. DOI: 10.1017/jfm.2016.172.

[40] P. Roache, "Verification and validation in computational science and engineering," *Journal of Computational Physics*, vol. 123, no. 4, pp. 567–589, 2009.

[41] S. Kallio, J. Peltola, and T. Niemi, "Analysis of the time-averaged gas-solid drag force based on data from transient 3d cfd simulations of fluidized beds," *Powder Technology*, vol. 274, pp. 227–238, Apr. 2015, ISSN: 1873328X. DOI: 10.1016/j.powtec.2015.01.029.

[42] J. Sodja, *Turbulence Models in CFD*. University of Ljubljana, 2007.

[43] V. Makarashvili, E. Merzari, A. Obabko, P. Fischer, and A. Siegel, "Accelerating the high-fidelity simulation of turbulence: Ensemble averaging," ASME, 2016. [Online]. Available: http://asmedigitalcollection.asme.org/FEDSM/proceedings-

pdf / FEDSM2016 / 50299 / V01BT26A003 / 2385220 / v01bt26a003 - fedsm2016 - 7853.pdf.

[44] R. Tosi, *Towards stochastic methods in cfd for engineering applications [ph.d thesis]*, Nov. 2021.

[45] K. Gordiz, D. J. Singh, and A. Henry, "Ensemble averaging vs. time averaging in molecular dynamics simulations of thermal conductivity," *Journal of Applied Physics*, vol. 117, 4 Jan. 2015, ISSN: 0021-8979. DOI: 10.1063/1.4906957.

[46] Y. Yamamoto, "Mathematical methods," in National Institute of Informatics, 2024.

[47] B. Galanti and A. Tsinober, "Is turbulence ergodic?" *Physics Letters, Section A: General, Atomic and Solid State Physics*, vol. 330, pp. 173–180, 3-4 Sep. 2004, ISSN: 03759601. DOI: 10.1016/j.physleta.2004.07.009.

[48] P. Bartholomew, G. Deskos, R. A. Frantz, F. N. Schuch, E. Lamballais, and S. Laizet, "Xcompact3d: An open-source framework for solving turbulence problems on a cartesian mesh," *SoftwareX*, vol. 12, Jul. 2020, ISSN: 23527110. DOI: 10.1016/j.softx.2020.100550.

[49] S. Laizet, "Incompact3d: A powerful tool to tackle turbulence problems on supercomputers," T. Kvamsdal, Ed., 2014. [Online]. Available: http://www3.imperial.ac.uk/tmfc/people/sylvainlaizet/.

[50] S. Laizet and E. Lamballais, "High-order compact schemes for incompressible flows: A simple and efficient method with quasi-spectral accuracy," *Journal of Computational Physics*, vol. 228, pp. 5989–6015, 16 Sep. 2009, ISSN: 10902716. DOI: 10.1016/j.jcp.2009.05.010.

[51] J. Jiménez and P. Moin, "The minimal flow unit in near-wall turbulence," *Journal of Fluid Mechanics*, vol. 225, pp. 213–240, 1991. DOI: 10.1017/S0022112091002033.

[52] S. B. Pope, *Turbulent Flows*. Cambridge University Press, 2000.

[53] C. D. Daniel, S. Laizet, and J. C. Vassilicos, "Wall shear stress fluctuations: Mixed scaling and their effects on velocity fluctuations in a turbulent boundary layer," 2017.

[54] N. G. R. Center, *Reynolds number*, 2024. [Online]. Available: https://www.grc.nasa.gov/www/k-12/airplane/reynolds.html.

[55] M. Lee and R. D. Moser, "Direct numerical simulation of turbulent channel flow up to," *Journal of Fluid Mechanics*, vol. 774, pp. 395–415, Jul. 2015, ISSN: 0022-1120. DOI: 10.1017/jfm.2015.268.

[56] L. Könözsy, *Navier Stokes Hypothesis for Newtonian Viscous Fluids [Course Notes]*, Canvas Cranfield, 2023.

[57] L. Könözsy, *Numerical Methods for Incompressible Flows [Course Notes]*, Canvas Cranfield, 2024.

[58] S. Laizet, *XCompact3d Introduction [Course Slide]*, Xcompact3d Course, 2024.

[59] D. G. Westra and J. C. Heinrich, *The fractional step method applied to simulations of natural convective flows*, 2002.

[60] D. R. Durran, "The third-order adams-bashforth method: An attractive alternative to leapfrog time differencing," *Monthly Weather Review*, vol. 119, pp. 702–720, 3 1991.

[61] G. H. Yeoh and J. Tu, "Solution methods for multi-phase flows," in Elsevier, 2010, pp. 95–242. DOI: 10.1016/B978-0-08-046733-7.00003-5.

[62] Ansys, *ANSYS Fluent Mosaic Technology Automatically Combines Disparate Meshes with Polyhedral Elements for Fast, Accurate Flow Resolution [White Paper]*, 2020.

[63] J. Tu, G.-H. Yeoh, and C. Liu, "Chapter 4 - cfd mesh generation: A practical guideline," in *Computational Fluid Dynamics (Third Edition)*, J. Tu, G.-H. Yeoh, and C. Liu, Eds., Third Edition, Butterworth-Heinemann, 2018, pp. 125–154, ISBN: 978-0-08-101127-0. DOI: https://doi.org/10.1016/B978-0-08-101127-0.00004-0. [Online]. Available: https://www.sciencedirect.com/science/article/pii/B9780081011270000040.

[64] A. Cain, J. Ferziger, and W. Reynolds, "Discrete orthogonal function expansions for non-uniform grids using the fast fourier transform," *Journal of Computational Physics*, vol. 56, pp. 272–286, 2 Nov. 1984, ISSN: 00219991. DOI: 10.1016/0021-9991(84)90096-2.

[65] E. J. Avital, N. D. Sandham, and K. H. Luo, "Stretched cartesian grids for solution of the incompressible navier-stokes equations," *International Journal for Numerical*

24

Methods in Fluids, vol. 33, pp. 897–918, 6 Jul. 2000, ISSN: 02712091. DOI: 10.1002/ 1097-0363(20000730)33:6<897::AID-FLD37>3.0.CO;2-4.

APPENDIX

A   Software Choice

Software	Advantages	Disadvantages
Incompact3d	DNS is default	Code structure is harder to read, harder interface
	Written in Fortran, less time to familiarise	Hard to find the documentation, contact must be done through Prof. Laizet
	Collaboration with Ricardo	
OpenFOAM	Code structure is easier to read, better interface	Written in C++, requires additional familiarisation time
	Documentation and guidance is already provided by Tom, easier contact if confused	DNS is harder to set up (requires dnsFoam), a lot of files to set up
		No collaboration?